Effect of applied interparticle force on the static and dynamic angles of repose of spherical granular material

A. J. Forsyth,[1] S. R. Hutton,[2] M. J. Rhodes,[1] and C. F. Osborne[2]

[1]*Department of Chemical Engineering, Monash University, Victoria 3800, Australia*
[2]*Department of Physics, Monash University, Victoria 3800, Australia*

The static angle of repose for iron spheres in a narrow box, and the dynamic angle of repose for iron spheres in a narrow, half-filled rotating drum is investigated. A feature of this paper is the use of a homogenous magnetic field to induce an attractive interparticle force, allowing a wide range of angles of repose to be investigated and characterized as a function of interparticle force. The static and dynamic angles of repose were found to increase approximately linearly with increasing interparticle force.

I. INTRODUCTION

A sandcastle is a particle technology laboratory. Ideally, we would like our structure to last until we decide to jump on it, or until the incoming tide washes it away. Experience quickly teaches us that damp sand is a much better building material than dry sand or very wet sand, especially if the castle is to have steeply sloped (or vertical) sides.

If one attempts to use dry sand, the sandcastle will have gently sloping sides, usually less than $25°$. Gravity is attempting to flatten the pile, and the only force resisting this is the weak interparticle friction. Adding water to the sand provides an interparticle force in the form of liquid bridges. It is this interparticle force that allows the sand to form structures with steep sides. This paper examines the effect of interparticle force on the angle of repose. We shall examine both the static and dynamic angles of repose, described in detail below.

When a powder is poured onto a flat plate, it forms a cone. Once the powder has reached an equilibrium state, the angle the sides of the cone make with the plate is called the static angle of repose. The angle of repose depends on such factors as size, density, surface roughness, and level of moisture of the powder, and the surface roughness of the plate. The static angle of repose can be measured in other ways, though not all methods will give the same angle of repose. For instance, a flat bottomed box can be filled, and the powder allowed to flow out through a hole in the bottom of the box. The angle that the remaining powder forms with the horizontal, once flow has ceased, is the static angle of repose. Other methods also exist, but this paper concentrates on the first method described here, the so-called ''poured'' angle of repose.

In addition, we shall consider the dynamic angle of repose, obtained as follows. A thin cylinder is half-filled with powder and placed on a pair of rollers. While stationary, the powder forms a flat surface inside the drum. As slow rotation begins, the material is carried along with the motion of the drum until the maximum angle of stability (the highest angle at which the surface of the powder is still in equilibrium) is exceeded. An avalanche ensues and the powder slumps to a new, lower angle of repose.

As the rotational speed increases, the avalanches increase in frequency until the surface of the powder is in constant motion, with a well-defined angle of repose. This will be referred to as the dynamic angle of repose. If one continues to increase the rotational speed, the surface of the powder takes on the characteristic S shape seen in Fig. 1.

The cohesive properties of powders depend on factors such as size, density, surface roughness, presence of liquid, and degree of compaction. Rather than examine each of these variables in isolation, we shall use the widely suggested idea that competition between the interparticle forces and the inertial forces determines granular behavior. As the ratio of interparticle force to inertial forces increases, the powder becomes more cohesive and the angle of repose increases accordingly.

For smooth dry powders, the dominant interparticle force is the van der Waals interaction. This increases linearly with particle size, while inertial forces increase as the cube of the particle size. Hence, the effect of the van der Waals force is best seen for small particles. For instance, coarse dry beach sand is free flowing, and forms piles with a very low angle of repose. On the other hand, fine powders such as corn flour and icing sugar are typically cohesive, and piles of these
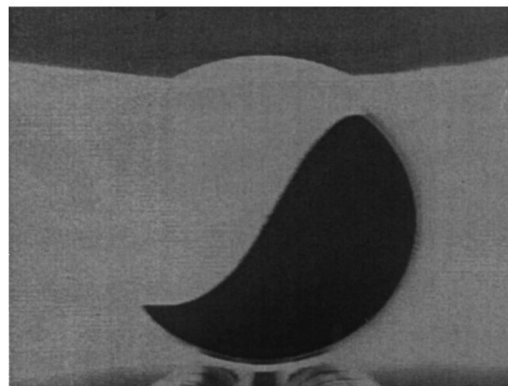

FIG. 1. Typical ''Ying-Yang'' shaped interface for a powder in a rotating drum at high rotational velocities. A threshold function was used to clearly delineate the powder surface. The aluminium rollers can be seen at the bottom of the picture. The dark bands at the top and bottom of the picture are the coils.

materials can support more steeply sloped sides.

Compaction will also have the effect of making a powder more cohesive. The van der Waals interaction for macroscopic particles falls off as the square of the interparticle separation [1]. Compaction decreases the average interparticle distance and hence increases the van der Waals force. In addition, compacting the powder increases the ''coordination number'' of the particles within the powders. For example in a loosely packed powder each particle may on average be in close contact with only 6 other particles, whereas in a closely packed state, they may be in contact with 8 to 12 particles, 12 representing the (in practice unattainable) hexagonal close-packed state.

The addition of liquid to dry powders will cause a transition in behavior. Experience shows that damp sand is better for making sandcastles than dry sand, due to its cohesive properties. The interparticle force in this case is caused by the formation of liquid bridges. Several groups [2,3] have added liquids of varying surface tensions and viscosities to dry powders to observe the transition from noncohesive to cohesive behavior.

To examine in detail this transition from noncohesive to cohesive behavior, a method for varying the ratio of interparticle force to inertial forces is needed. We shall discuss briefly methods used previously and note the disadvantages associated with each.

As discussed above, one may change the ratio of interparticle force to inertial force by altering the particle size. This leads to several complications. For instance, particles might not be available in the size you desire. Commercial batches of say 250 and 500 μm may not have the same relative size distribution. Most importantly however, it is difficult to obtain the same initial experimental conditions with different particle sizes. It is well known [4] that while particles larger than approximately 250 μm pack under normal gravity with roughly the same voidage, for particles smaller than this the voidage increases with decreasing particle size.

Liquid bridges can be used to increase the interparticle force. Several groups [2,3,5] have added liquids of varying surface tensions and viscosities to dry powders to observe the increase in interparticle force. Work has also been done on examining the effect of liquid on packing of monosized coarse spheres [4]. The limitation of this method is that the addition of more and more liquid increases the interparticle force in a stepwise manner. It is difficult to remove liquid in a controllable way. Adding liquids to dry powders not only increases the interparticle interaction, but also the interaction between the powder and the wall, further complicating the analysis. It is well known that the walls of a container can support a large fraction of the weight of the powder inside. For angle of repose experiments such as those performed here, this will increase the angle of repose, as part of the weight is supported by the walls, rather than by the pile of powder. Perhaps most importantly, it is difficult to relate the quantity of liquid added to the interparticle force.

To avoid these complications, we have examined the packing of iron spheres within a magnetic field. Varying the strength of the field allowed us to continuously vary the resulting interparticle magnetic force. As the walls of the ves-

sel are nonmagnetic perspex, the particle-wall interaction is unchanged. As the same particles under the same packing conditions are used for all of the experiments, it is ensured that the initial conditions are as uniform as possible.

If it is assumed that the particles are magnetically linear, it follows that the interparticle force between two particles F_{mag} will vary in proportion to the square of the applied magnetic field ($F_{\mathrm{mag}} \approx B_0^2$) [6]. Rather than rely on a calculation of the field from theory, we measure the ratio of interparticle force to buoyant weight directly, as described below. A plot of measured force against field strength squared was approximately linear, and we were confident in preparing a linear calibration curve to allow us to determine the interparticle force to buoyant weight ratio for any given field strength.

II. EXPERIMENTAL APPARATUS

To measure the static angle of repose, a narrow rectangular box of width 4 mm, length 300 mm, and height 150 mm was filled with iron spheres of mean diameter 800 μm from a funnel with a stopcock attached. The stopcock was used to control the flow rate.

To measure the dynamic angle of repose, a narrow perspex drum of diameter 150 mm and thickness 10 mm was placed horizontally on a set of aluminum roller supports and driven by an electric motor. Due to the presence of the magnetic field, only nonmagnetic materials were used in construction of the roller supports, and these were connected to the electric motor via a long belt. The drum was approximately half-filled with iron spheres.

The magnetic field for this experiment is supplied by a pair of Helmholtz coils. These coils have an inner diameter of 456 mm, an outer diameter of 568 mm, and a thickness of 76 mm. The formers are constructed from nylon, and were each wound with 1.1 km of 2.240 mm diam insulated copper wire. The coils are powered by a 16 A, 16 V stabilized dc power supply, and have a total resistance of 2.2 Ω. Thermal sensors on the inner wall of the coils provide information about temperature within the coils. If the temperature rises above a preset value, the power supply will automatically switch off. Additional cooling can be provided by a water jacket, but was not found to be necessary for these particular experiments. The magnetic-field axis was in the vertical direction.

The magnetic field was measured as a function of current by a Bell 2400 series Gaussmeter. The field was found to vary less than 10% throughout the volume between the coils, and by less than 5% within a sphere of diameter 140 mm centered on the axis of symmetry, midway between the coils. The variation in magnetic-field intensity with current is shown in Fig. 2.

To directly measure the interparticle force between two particles as a function of field strength, the following method was used. An iron sphere of the appropriate size was glued to a plastic spatula and positioned on the axis of symmetry at the point midway between the coils. With the field at full strength (approximately 6400 A/m) a second particle of the same size was brought into contact with the fixed sphere.
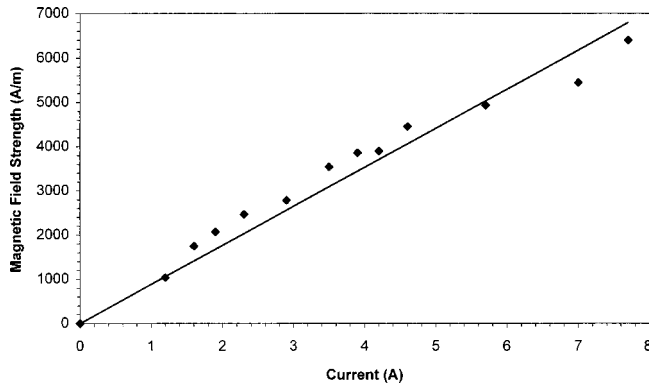
FIG. 2. Variation of magnetic-field intensity with current. The measurements were taken along the axis of symmetry, midway between the coils.

Due to the strong magnetic force between the two particles, the second particle became suspended from the first. The current in the coils, and hence the magnetic-field strength was slowly decreased until the suspended particle fell from the fixed particle. At this point the interparticle force is equal to the weight of the particle. This measurement (and all subsequent measurements) were repeated several times for accuracy. The weight of the particle was measured with a sensitive laboratory balance.

To obtain further points for the graph, small (500 μm) bronze spheres were carefully glued to the ''bottom''of the particle to be suspended. This served to increase the weight of the particle without significantly altering the interparticle force. This new particle was weighed, and the measurements repeated, making sure that none of the bronze particles became dislodged when the suspended particle fell. The weight of the particle versus the square of the field at which it fell is shown in Fig. 3. By dividing through by the weight of each particle, we can obtain the ratio of interparticle force to weight, as shown on the right-hand axis of Fig. 3.

Ramping the field down slowly serves two purposes. First of all, it allows us to pinpoint the current and hence field at which the interparticle force and gravitational forces become equal. Secondly, it allows the magnetic field induced in the steel spheres to relax, so that the force is representative of the present field, rather than the higher field it was at moments ago.
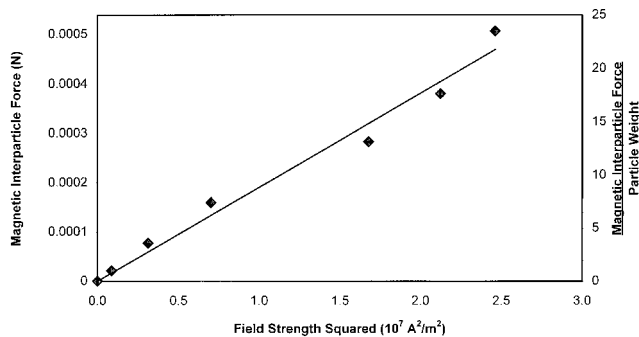

FIG. 3. Graph of interparticle force and interparticle force per unit weight vs magnetic-field strength squared for 800-μm steel spheres.
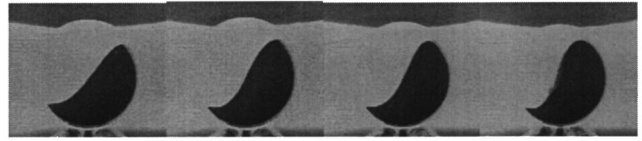

FIG. 4. Typical curves of the type analyzed in this paper. From left to right the figures represent a ratio of interparticle force to weight of 0, 0.62, 5.6, and 10, respectively.

An image recognition system consisting of a commercial digital camera attached to a Matrox card was used to capture the images and our own software used to analyze the results. Lighting was controlled by back lighting, using a diffuser to ensure uniformity of the lighting conditions. Preprocessing to remove noise and unwanted artifacts was applied to all images.

A set of experiments were conducted to measure the angle of repose for different values of interparticle force.

III. RESULTS

The increase in dynamic angle of repose with increasing interparticle force can be clearly seen in Fig. 4. The angle of repose was determined by first segmenting the image, and the angles were determined using a Hough transform. This approach is robust to noise and is preferred to other curve-fitting techniques [7].

The results of the experiments to measure the static and dynamic angles of repose are shown in Figs. 5 and 6. In both cases, the angle of repose increases approximately linearly with increasing interparticle force. Similar results for the static angle of repose have been demonstrated elsewhere [2,3,8] for liquid bridge forces, using the ''draining crater'' [2] method to measure the angle of repose.

This linear behavior corresponds to the *granular regime* of Tegzes *et al.* [8] for wet granular media, where surface flow is homogenous and involves only the top few layers of grains. This behavior manifests itself at low level of liquid addition. As the amount of liquid increases, two other regimes have been discovered. In the *correlated regime* surface flow becomes strongly correlated in that clumps of many attached grains fall in each avalanche, leading to a
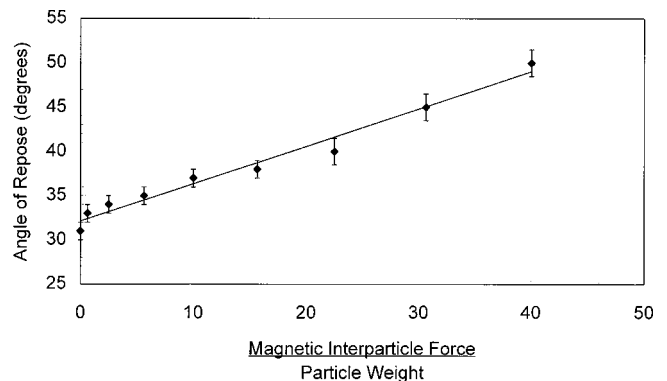

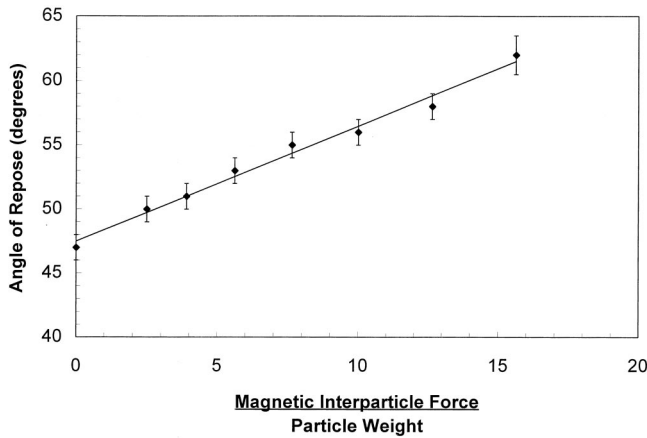FIG. 5. Graph of static angle of repose vs ratio of interparticle force to weight for 800-μm steel spheres.

FIG. 6. Graph of dynamic angle of repose vs ratio of interparticle force to particle weight for 800-μm steel spheres.

cratered surface. In this regime the angle of repose rises more slowly than in the *granular regime*, though still in a somewhat linear manner. In the *plastic regime* surface flow is reminiscent of a viscous fluid in that the surface remains smooth, rather than taking on the cratered appearance that appears in the *correlated regime*. In the *plastic regime* the angle of repose stops increasing with additional liquid content, and indeed in some cases actually decreases.

It is unclear whether correlated and plastic regimes will show up at higher fields. Obviously the angle of repose cannot continue to increase linearly with increasing field, as the angle of repose cannot exceed 90°, and one doubts whether in practice this can even be approached closely. At high fields, the poured angle of repose becomes difficult to measure due to the cohesive nature of the iron spheres. The iron spheres begin to ''clump,'' blocking the orifice in the funnel. Further experiments are planned using the ''draining crater'' method to search for these other regimes.

IV. DISCUSSION

Theoretical studies based on stability criteria [2] demonstrate that the maximum angle of stability should increase approximately linearly with increasing interparticle force from about 23° at zero interparticle force up to a little over 80° at a ratio of interparticle force to weight of 1. At ratios above 1 the graph tails off towards the maximum angle of repose at 90°. The work of Albert *et al.* [2] considered liquid bridge forces as the interparticle cohesive force. The theory is based on the maximum angle of stability for stationary particles, rather than the poured angle of repose measured here. In essence, this corresponds to taking a flat surface of particles and very slowly tilting it until flow begins. The particles in this experiment have been dropped from an average height of around 10 cm, and gain a velocity of the order of 1 ms^{-1} before impacting on the surface of the pile. This energy must be dissipated before the particle comes to rest, and obviously allows the particle to come to rest further down the slope than it would if it were placed gently at the top of the pile.

It is perhaps not surprising that the angles of repose mea-

sured here rise more slowly with increasing interparticle force than theory based on liquid bridge forces would suggest. One limitation of the system used here is that the force is a dipole interaction rather than an isotropic force such as the van der Waals force. Not only is the magnetic force anisotropic, but particles situated next to one another (in the same horizontal plane) will actually repel one another. If we assume the pile is packed in a cubic state, all particles on the surface of the pile will have a neighbor on the same plane up slope, but not necessarily corresponding neighbor down slope. This results in a net force F_{cub} attempting to push the particle further down the slope, lowering the angle of repose. If the packing was perfectly hexagonal close packed, the net horizontal force on a particle at the surface would be zero. In practice, the packing is random, and the net horizontal force on particles at the surface somewhere between zero and F_{cub}.

Additionally, we have quoted here only the maximum interparticle force F_{max}, obtained when the particles are touching and aligned with the field. It is easily demonstrated [1] that (at least for separations large compared to the dimensions of the dipole) that the interaction energy for particles aligned in the direction of the field is twice that of two dipole aligned parallel to each other at the same separation. When the line joining the centers of our particles is aligned with the field, our dipoles attract and repel when the line joining the centers of the particles is perpendicular to the field lines. The average force felt by the particles will overall be attractive, but less than F_{max}. Hence our ratio of interparticle force to particle weight is overestimated.

The liquid bridge force is also anisotropic. The liquid bridge force is always attractive, and acts along a line joining the centers of two particles. This results in a net horizontal force towards the slope, rather than away from the slope as in the magnetic case. One would therefore expect that the angle of repose for wet powders would increase more rapidly as a function of the ratio of interparticle force to particle weight than the magnetic case, and so perhaps better reflect the theory of Albert *et al.* [2]

It is difficult to quantitatively compare our data to those experiments done using liquid bridges to supply the interparticle force as there is at this stage no robust manner in which to calculate the interparticle force due to liquid bridges without resorting to fitted parameters. The work of Hornbaker *et al.* [3] plots a static angle of repose obtained by the draining-crater method [9] versus the average liquid layer thickness. The angle of repose rises approximately linearly with increasing liquid layer thickness. Albert *et al.* [2] demonstrate that for slightly rough particles, the liquid bridge force $F_{liq} \approx V^{1/3}$, where V is the volume of the liquid bridge. Hence, liquid bridge interparticle force is proportional to the thickness of the liquid layer. Qualitatively, this gives the same behavior seen using magnetic forces, that angle of repose increases linearly with increasing interparticle force.

Basic stability criteria [2] would predict an angle of repose at a zero field of approximately 23°. Our angle of repose is significantly higher ($\approx 31°$). The difference can possibly be attributed to the narrow box used for the experiments. It is well known that wall effects can add sev-

eral degrees to the angle of repose [10]. Repeating our experiments at zero field with boxes of width 6 mm and 8'mm gave angles of repose of 30° and 28°, respectively. Zero-field experiments were performed on iron spheres that had not previously been magnetized to ascertain whether residual magnetization was the cause. No effect due to residual magnetization was found.

The dynamic angle of repose at zero field (47°) is considerably higher than the static angle of repose at zero field (31° for the 800-μm particles). The motion of the drum carries the particles up the wall, leading to a higher angle of repose. As for the static case, the dynamic angle of repose rises linearly with increasing interparticle force, though more slowly than predicted by theory [2] due to the inertia of the particles.

V. CONCLUSIONS

We have designed a system for examining the effects of interparticle force on the behavior of powders. The static angle of repose for iron spheres in a box and the dynamic angle of repose for iron spheres in a rotating drum were measured as a function of interparticle force. Both the static and dynamic angles of repose were found to increase approximately linearly with interparticle force.

[1] J.N. Israelachvili, *Intermolecular and Surface Forces*, 2nd ed. (Academic, San Diego, 1992).

[2] R. Albert, A. Istvan, D. Hornbaker, P. Schiffer, and A.-L. Barabasi, Phys. Rev. E **56**, R6271 (1997).

[3] D.J. Hornbaker, I. Albert, A.L. Barabasi, and P. Schiffer, Nature (London) **387**, 765 (1997).

[4] C.L. Feng and A.B. Yu, Powder Technol. **99**, 22 (1999).

[5] L.J. McLaughlin and M.J. Rhodes, Powder Technol. **114**, 213 (2001).

[6] T.B. Jones, R.D. Miller, K.S. Robinson, and W.Y. Fowlkes, J. Electrost. **22**, 231 (1989).

[7] R.C. Gonzalez and P. Wintz, *Digital Image Processing*, 2nd ed. (Addison-Wesley, Reading, MA, 1987).

[8] P. Tegzes, R. Albert, M. Paskvan, A.-L. Barabasi, T. Vicsek, and P. Schiffer, Phys. Rev. E **60**, 5823 (1999).

[9] R.L. Brown and J.C. Richards, *Principles of Powder Mechanics* (Pergamon, Oxford, 1970).

[10] C.M. Dury, G.H. Ristow, J.L. Moss, and M. Nakagawa, Phys. Rev. E **57**, 4491 (1998).